International Tables for X-ray Crystallography (1968). Tome III. Birmingham: Kynoch Press.

LAVAL, J. P., MERCURIO-LAVAUD, D. & GAUDREAU, B. (1974). *Rev. Chim. Minér.* **11**, 742–750.

O'KEEFFE, M. & HYDE, B. G. (1980). *Phil. Trans. R. Soc. London, Ser. A*, **295** (1417), 553–618.

PAPIERNIK, R., FRIT, B., LAVAL, J. P. & GAUDREAU, B. (1981). En préparation.

POULAIN, M., POULAIN, M. & LUCAS, J. (1973). *J. Solid State Chem.* **8**, 132–141.

SEARS, D. R. & BURNS, J. H. (1964). *J. Chem. Phys.* **41**, 3478–3483.

SHELDRICK, G. M. (1976). *SHELX* 76. Programme pour la détermination de structures cristallines. Univ. Cambridge, Angleterre.

WELLS, A. F. (1975). *Structural Inorganic Chemistry*, 4e éd., pp. 68–69, 359–362. Oxford: Clarendon Press.

Acta Cryst. (1982). B**38**, 2353–2357

Structure (Neutron) of Phase IV Rubidium Nitrate at 298 and 403 K

BY M. SHAMSUZZOHA AND B. W. LUCAS

Department of Physics, University of Queensland, St Lucia, Brisbane, Queensland 4067, *Australia*

(*Received* 3 *November* 1981; *accepted* 1 *April* 1982)

Abstract

The crystal structure of phase IV $RbNO_3$ has been determined at room temperature (298 K) and, closer to the IV → III transition, at 403 K by three-dimensional single-crystal neutron diffractometry. The crystal system is trigonal, space group $P3_1$ (or its enantiomorph $P3_2$), with $a = 10{\cdot}55$ (2), $c = 7{\cdot}47$ (2) Å at 298 K and $a = 10{\cdot}61$ (1), $c = 7{\cdot}55$ (1) Å at 403 K, and $Z = 9$. The single-crystal neutron diffraction intensity data for 298 K were severely affected by extinction. Inclusion of anisotropic extinction correction and anisotropic temperature factors in the least-squares refinement of 1080 reflections (equivalents, not averaged) gave a converged conventional R-factor value of 0·068. The least-squares refinement for 451 independent reflections of 403 K intensity data, with isotropic extinction correction and anisotropic temperature factors, gave a converged conventional R factor value of 0·078. The structure, at both temperatures, has the Rb atoms forming a pseudocubic sublattice with nine pseudocubes per unit cell. The NO_3-groups' configurations within the unit cell are derived from an asymmetric unit of three NO_3 groups. Average N–O distances and O–N̂–O angles are 1·25 (1) Å and 119 (1)° at 298 K, and 1·20 (1) Å and 119 (2)° at 403 K. Each NO_3 group is essentially parallel to one of the faces of its surrounding Rb-atom pseudocube and one of the N–O bonds is also almost parallel to a pseudocube cell edge.

Introduction

At atmospheric pressure, $RbNO_3$ undergoes the following thermal polymorphic phase transitions (Plyuschev, Markina & Shklover, 1956; Brown & McLaren, 1962):

$$RbNO_3(IV) \xrightarrow{437\ K} RbNO_3(III) \xrightarrow{492\ K} RbNO_3(II) \xrightarrow{564\ K} RbNO_3(I).$$

The $RbNO_3$(IV) crystal structure has been investigated previously by X-ray diffraction single-crystal methods. Pauling & Sherman (1933) reported the crystal data as: trigonal, $a = 10{\cdot}45$, $c = 7{\cdot}38$ Å, $Z = 9$, Laue group $\bar{3}m$, space group $P31m$. Brown & McLaren (1962) also reported the Laue group to be $\bar{3}m$, but the space group as $P3_112$ (or its enantiomorph $P3_212$) with cell dimensions $a = 10{\cdot}48$, $c = 7{\cdot}45$ Å and $Z = 9$. The observed presence of pyroelectricity along the crystallographic c axis (Bury & McLaren, 1969) and optical activity (Karpov & Shultin, 1970), however, suggested the point group to be 3 and Laue group $\bar{3}$. Hence, the Laue group could not be uniquely assigned, remaining as either $\bar{3}$ or $\bar{3}m$, and no complete crystal structure had been reported.

In order to resolve the above ambiguity, the present determination of the crystal structure for $RbNO_3$(IV) was made. Owing to the considerably larger X-ray scattering power of Rb atoms compared to the NO_3-group atoms, previous X-ray diffraction measurements yielded only limited information regarding the orientation of the NO_3 group in the unit cell. The coherent neutron scattering lengths of Rb, N, and O are comparable, and so single-crystal neutron scattering techniques were employed for the present experimental data collection. Besides making a room-temperature determination, it was decided to make a determination just below the IV → III transition as an aid to the understanding of the transition.

0567-7408/82/092353-05$01.00

Experimental

Single crystals of $RbNO_3$(IV) were grown by slow evaporation of an aqueous solution at room temperature ($RbNO_3$ powder of stated purity 99·8% from Koch-Light Laboratories, England, was used).

The two single-crystal specimens, one for each temperature (298 and 403 K), used for the neutron diffraction studies were close to hexagonal-shaped needles of approximate dimensions 0·25 × 1·5 × 3 mm and 0·65 × 3·0 × 5·8 mm respectively. Each crystal was mounted with its c axis almost parallel to the φ axis of a computer-controlled four-circle neutron diffractometer, one diffractometer belonging to the Australian Institute of Nuclear Science and Engineering (AINSE) and the other to the Australian Atomic Energy Commission (AAEC); both were installed at the Australian Atomic Energy Commission (AAEC) research reactor HIFAR, at Lucas Heights. The crystal used in the 403 K study was heated by a single-crystal neutron diffraction furnace (Lucas, 1976). A thermocouple attached to the crystal at its support point gave the sample temperature (variation of which was ±1 K).

The wavelengths used were 1·705 Å (Ge monochromator) for the 298 K study, and 1·249 Å (graphite monochromator) at 403 K. For measurement of the integrated intensities, ω–2θ scans (with a 2θ step size of 0·01° and width of 2·2°) were used at each temperature. Background–peak–background measurements were made for each Bragg reflection. A standard reflection (412) was monitored after every 25 reflections at each temperature. There were no significant variations in the magnitude of this standard. Equivalent sets of Bragg intensities (for half of the reciprocal-space sphere, $l \geq 0$) out to a limit of $\sin\theta/\lambda \leq 0{\cdot}455$ and $\sin\theta/\lambda \leq 0{\cdot}488$ Å^{-1} were collected for 298 and 403 K, respectively.

While heating the specimen (at a rate of 5 K h^{-1}) from room temperature, for the proposed single-crystal neutron data collection at 403 K, the integrated intensities of some strong, low-index reflections, *e.g.* 300, $1\bar{1}1$, $\bar{2}\bar{2}2$, were found to *increase* gradually to maxima values at around 353 K and then decrease gradually with further temperature rise (Fig. 1). This contrasts with the fact that the observed intensities *normally reduce with temperature rise* (due to the Debye–Waller temperature factor).

Analysis

The cell dimensions (see *Abstract*) obtained from X-ray oscillation and Weissenberg photographs at room temperature and from the single-crystal neutron diffractometry data collected at 403 K were used in the following analysis.

The values of integrated intensities I (reflections greater than 1σ were considered as observed), and $\sigma(I)$, in the neutron data set for both temperatures were corrected for absorption effects (μ = 0·03955 mm^{-1}). An examination of the 298 K absorption-corrected data revealed that the intensities associated with the set of crystallographic planes (*hkil*), for cyclic permutation of *hki*, had equal magnitudes within the counting statistics. Similar equality within the set of (*khil*), for cyclic permutation of *khi*, was also apparent. However, comparison of intensity magnitudes between these sets left some uncertainty in the assignment of the Laue group: equality would have indicated $\bar{3}1m$ (Nimmo, 1980), while inequality would give $\bar{3}$. Similar examination of the 403 K absorption-corrected data determined the Laue group uniquely as 3, at this temperature.

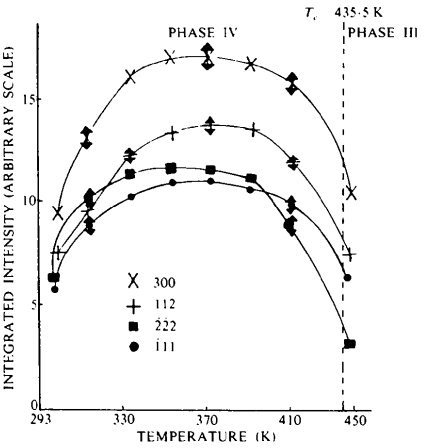

(*a*)

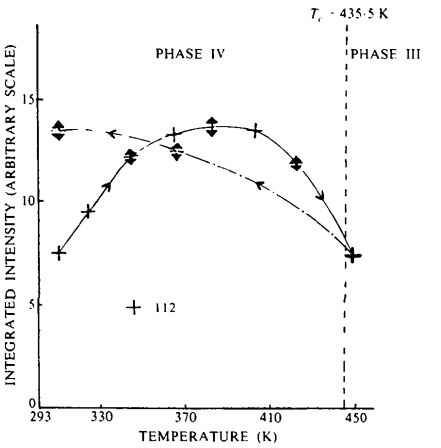

(*b*)

Fig. 1. (*a*) Variation of integrated intensities for some strong, low-index reflections of $RbNO_3$(IV), with temperature increase. (*b*) Variation of the integrated intensity for reflection 112 of $RbNO_3$(IV), over a temperature cycle.

In order to define the reliability of the data, statistical analyses were performed (F test at the 1% level) for the above-mentioned Laue groups' symmetry-related reflections. These analyses led to rejection of more than one third of the total number of reflections in the data for the Laue group $\bar{3}1m$, whereas only a few symmetry-related reflections, *i.e.* $\bar{1}\bar{1}1$, 300, $\bar{2}\bar{2}2$, $\bar{1}\bar{4}4$ and 330 for 298 K, and 300 for 403 K, were rejected for the Laue group $\bar{3}$ data. Lorentz-factor corrections were applied to all statistically reliable reflections and finally the symmetry-related reflection intensities were averaged. The numbers of independent reflections thus obtained were 167 (Laue group $\bar{3}1m$), 371 (Laue group $\bar{3}$ for 298 K) and 451 (Laue group $\bar{3}$ for 403 K).

The observed piezoelectricity (Hettich & Steinmetz, 1932) and pyroelectricity along the crystallographic c axis (Bury & McLaren, 1969), in conjunction with the crystallographic data, require the point-group symmetry to be 3 or $3m$. Although the observed optical activity (Karpov & Shultin, 1970) is not consistent with the point group $3m$, the possibility of Laue group $\bar{3}1m$ for the 298 K data suggested that this point group should not be excluded from the analysis at this stage. The space groups belonging to the point group $3m$ (and the Laue group $\bar{3}1m$) are $P31m$, $P31c$, $R3m$, $R3c$. The systematic absences, $00l$ for $l \neq 3n$, in the neutron data eliminated all except $P31m$ (which was accepted on the assumption that the mentioned absences were by chance).

A few possible structures, which could be fitted to the space group $P31m$, were tried, but without success. This suggested that the appearance of a mirror plane through the threefold axis on some preliminary X-ray Laue photographs had probably been a pseudo mirror and the analysis of the 298 K neutron data should be based on the Laue group $\bar{3}$. The point group 3, belonging to the Laue group $\bar{3}$, has the possible space groups $P3$, $R3$, $P3_1$ (or its enantiomorph $P3_2$). The systematic absences, $00l$ for $l \neq 3n$, eliminated all except $P3_1$ (or its enantiomorph $P3_2$).

A proposed (X-ray-determined) crystal structure (Kennard, 1978) with the space group $P3_1$ was used as an initial model structure, although its NO_3 groups were considerably distorted from their usually accepted configuration. A Fourier synthesis with 125 strongest (room-temperature) neutron intensity reflections, phased by the proposed structure, yielded all the atoms in the unit cell as positive peaks, but with poor resolution. The atomic positions thus obtained were refined by a series of full-matrix least-squares refinements, using the complete neutron data set. The refinement was initially performed with isotropic temperature factors, but subsequently anisotropic temperature factors and an isotropic extinction factor were introduced; the function minimized was $\sum w(|F_o|^2 - |F_c|^2)^2$ and the weighting factor was $w(hkl) = \{\sigma^2[|F(hkl)|^2]\}^{-1}$. The coherent scattering lengths used were: Rb* = 7·1 fm (Franklin & Cox, 1970); N = 9·4 fm (*International Tables for X-ray Crystallography*, 1974); and O = 5·83 fm (Schneider, 1976).

The refinement converged, but an examination of the $|F_o|^2$ and $|F_c|^2$ values for the stronger reflections indicated that the single-crystal data were severely affected by extinction. Anisotropic extinction corrections were therefore introduced and used in the final cycles of the least-squares refinement. Consequently, a total of 1080 statistically reliable reflections (equivalents, not averaged) were employed in this refinement. The positional parameters for the anisotropic extinction model and the agreement factors at convergence are listed in Table 1.† The final structure was confirmed by Fourier and difference Fourier syntheses. For the Fourier maps, all the atomic positions appeared as well resolved peaks at essentially the least-squares-refined positions, while with the difference Fourier synthesis no significant peaks occurred.

A similar analysis also revealed the space group for the 403 K neutron data to be $P3_1$ (or its enantiomorph $P3_2$). The crystal structure from the 298 K neutron data was used as the initial model structure in the least-squares refinement. The scattering length of Rb* was introduced as an additional parameter to the positional, anisotropic thermal, and isotropic extinction parameters. The atomic positional parameters and the converged values of the agreement factors are listed in Table 1.† The structure was also confirmed by Fourier and difference Fourier syntheses.

The crystal structure at 298 and 403 K

The crystal structure (with space group $P3_1$) has the Rb atoms forming a pseudocubic sublattice with nine pseudocubes per unit cell. The NO_3-group configurations, within the unit cell, are derived from an asymmetric unit of three NO_3 groups (Fig. 2). The NO_3 groups are closely planar and each is enclosed by a pseudocube of Rb atoms. The plane of each NO_3 group is almost parallel to one of the faces of its enclosing pseudocube. The interatomic distances and interbond angles below 4 Å for 298 and 403 K are

* In final cycles of the least-squares refinements, 7·2 (2) fm was used for Rb, as obtained during the refinement of the 403 K single-crystal neutron data; this is because some discrepancies existed between values reported in the literature (Mueller, Sidhu, Heaton, Hitterman & Knott, 1963; Shull & Wollan, 1956; Franklin & Cox, 1970; Schneider, 1976).

† Lists of structure factors, anisotropic thermal parameters, and some information about the extinction effects have been deposited with the British Library Lending Division as Supplementary Publication No. SUP 36872 (31 pp.). Copies may be obtained through The Executive Secretary, International Union of Crystallography, 5 Abbey Square, Chester CH1 2HU, England.

Table 1. *Atomic positional parameters of* $RbNO_3$(IV) *as determined by least-squares refinement at* 298 *and* 403 K

Standard deviations are in parentheses and the parameter without a standard deviation was fixed to define the origin. $B_{eq} = \frac{4}{3} \sum_i \sum_j \beta_{ij} \mathbf{a}_i . \mathbf{a}_j$.

	At 298 K				At 403 K			
	x	y	z	B_{eq} (Å^2)	x	y	z	B_{eq} (Å^2)
Rb(1)	0·4566 (3)	0·5691 (3)	0·6236 (5)	3·03	0·4509 (7)	0·5627 (7)	0·6282 (9)	3·34
Rb(2)	0·1184 (3)	0·2192 (3)	0·0000	3·72	0·1174 (10)	0·2251 (9)	0·0000	5·05
Rb(3)	−0·2228 (4)	0·2214 (3)	0·6381 (6)	4·64	−0·2254 (7)	0·2184 (6)	0·6454 (17)	4·91
N(1)	0·4388 (4)	0·5668 (4)	0·1053 (6)	3·83	0·4432 (9)	0·5716 (8)	0·1099 (21)	4·04
N(2)	0·0962 (3)	0·2042 (3)	−0·4682 (6)	3·31	0·1022 (7)	0·2048 (5)	−0·4696 (19)	2·81
N(3)	−0·2580 (3)	0·2057 (3)	0·1168 (7)	3·31	−0·2544 (6)	0·2086 (5)	0·1450 (22)	3·92
O(1)	0·3371 (6)	0·5582 (5)	0·0094 (8)	5·00	0·3394 (12)	0·5597 (11)	0·0223 (25)	6·41
O(2)	0·3964 (5)	0·4704 (5)	0·2280 (8)	5·07	0·4121 (16)	0·4886 (12)	0·2283 (27)	8·36
O(3)	0·5646 (5)	0·6512 (5)	0·0664 (9)	5·38	0·5615 (10)	0·6584 (12)	0·0712 (24)	8·50
O(4)	−0·0011 (4)	0·1089 (4)	−0·3755 (7)	3·44	0·0042 (10)	0·1152 (9)	−0·3790 (23)	5·15
O(5)	0·2309 (5)	0·2495 (5)	−0·4363 (8)	4·94	0·2254 (11)	0·2458 (11)	−0·4284 (27)	8·06
O(6)	0·0581 (5)	0·2465 (5)	−0·6051 (8)	4·60	0·0763 (24)	0·2524 (17)	−0·6011 (22)	12·30
O(7)	−0·3078 (5)	0·1208 (5)	0·2503 (7)	4·49	−0·3221 (13)	0·1196 (13)	0·2577 (22)	7·51
O(8)	−0·1279 (6)	0·2774 (6)	0·0897 (8)	5·19	−0·1314 (11)	0·2699 (15)	0·1157 (27)	9·35
O(9)	−0·3459 (5)	0·2174 (5)	0·0140 (7)	4·55	−0·3305 (14)	0·2250 (12)	0·0281 (23)	7·61

	At 298 K	At 403 K		At 298 K	At 403 K
Number of variables	141	136	$R = \sum \lvert F_o^2 - F_c^2 \rvert / \sum \lvert F_o^2 \rvert$	0·114	0·080
Number of reflections	1080	451	$R_w = [\sum w(F_o^2 - F_c^2)^2 / \sum w(F_o^2)^2]^{1/2}$	0·135	0·082
	(371 non-equivalents)	(non-equivalents)	$R_1 = \sum \lvert \lvert F_o \rvert - \lvert F_c \rvert \rvert / \sum \lvert F_o \rvert$	0·068	0·078
Extinction correction	Anisotropic (type II)	Isotropic			

Table 2. *Interatomic distances* (Å) *and angles* (°) *for* $RbNO_3$(IV) *at* 298 *and* 403 K

Standard deviations are in parentheses. Superscripts i, ii, iii represent the equivalent positions x,y,z; $\bar{y}$, $x - y$, $\frac{1}{3} + z$; $y - x$, $\bar{x}$, $\frac{2}{3} + z$, respectively.

	At 298 K	At 403 K		At 298 K	At 403 K		At 298 K	At 403 K
Rb(1^i)···O(1^{ii})	3·11 (1)	3·13 (2)	Rb(2^i)···O(1^i)	3·14 (1)	3·13 (1)	Rb(3^i)···O(2^{ii})	2·95 (1)	3·04 (2)
Rb(1^i)···O(1^{iii})	3·12 (1)	3·13 (1)	Rb(2^i)···O(2^i)	3·28 (1)	3·44 (2)	Rb(3^i)···O(3^{iii})	2·98 (1)	3·11 (2)
Rb(1^i)···O(1^i)	3·12 (1)	3·20 (2)	Rb(2^i)···O(3^{iii})	3·17 (1)	3·10 (2)	Rb(3^i)···O(4^i)	3·11 (1)	3·14 (2)
Rb(1^i)···O(2^i)	3·09 (1)	3·10 (2)	Rb(2^i)···O(4^{ii})	3·10 (1)	3·18 (1)	Rb(3^i)···O(5^{ii})	3·09 (1)	3·12 (2)
Rb(1^i)···O(2^{ii})	3·48 (1)	3·59 (2)	Rb(2^i)···O(4^{iii})	3·06 (1)	3·24 (2)	Rb(3^i)···O(6^i)	3·37 (1)	3·56 (3)
Rb(1^i)···O(3^{iii})	3·52 (1)	3·40 (2)	Rb(2^i)···O(4^i)	3·14 (1)	3·10 (2)	Rb(3^i)···O(7^i)	3·06 (1)	3·11 (2)
Rb(1^i)···O(3^i)	3·46 (1)	3·52 (2)	Rb(2^i)···O(5^{ii})	3·49 (1)	3·48 (2)	Rb(3^i)···O(7^{ii})	3·31 (1)	3·22 (2)
Rb(1^i)···O(5^i)	3·03 (2)	3·03 (1)	Rb(2^i)···O(5^i)	3·43 (1)	3·40 (2)	Rb(3^i)···O(8^{iii})	3·64 (1)	3·74 (2)
Rb(1^i)···O(6^{ii})	2·99 (1)	3·08 (2)	Rb(2^i)···O(6^{iii})	3·39 (1)	3·58 (2)	Rb(3^i)···O(8^i)	3·48 (1)	3·65 (2)
Rb(1^i)···O(7^{iii})	3·42 (1)	3·36 (2)	Rb(2^i)···O(6^i)	3·06 (1)	3·08 (2)	Rb(3^i)···O(9^{ii})	3·12 (1)	3·22 (2)
Rb(1^i)···O(8^{ii})	3·07 (1)	3·10 (2)	Rb(2^i)···O(7^{iii})	2·98 (1)	3·11 (2)	Rb(3^i)···O(9^{iii})	3·14 (1)	3·12 (2)
Rb(1^i)···O(9^{iii})	3·11 (1)	3·21 (1)	Rb(2^i)···O(8^i)	3·03 (1)	3·04 (2)	Rb(3^i)···O(9^i)	3·09 (1)	3·11 (2)
N(1^i)–O(1^i)	1·26 (1)	1·24 (2)	N(2^i)–O(4^i)	1·23 (1)	1·21 (2)	N(3^i)–O(7^i)	1·27 (1)	1·21 (2)
N(1^i)–O(2^i)	1·27 (1)	1·18 (2)	N(2^i)–O(5^i)	1·27 (1)	1·19 (1)	N(3^i)–O(8^i)	1·21 (1)	1·15 (1)
N(1^i)–O(3^i)	1·21 (1)	1·16 (1)	N(2^i)–O(6^i)	1·26 (1)	1·21 (2)	N(3^i)–O(9^i)	1·26 (1)	1·27 (2)
O(1^i)–N(1^i)–O(2^{ii})	114·0 (4)	115·3 (1·1)	O(4^i)–N(2^i)–O(5^i)	121·3 (5)	119·5 (1·5)	O(7^i)–N(3^i)–O(8^i)	121·0 (5)	129·9 (1·6)
O(1^i) N(1^i)··O(3^i)	120·1 (5)	120·0 (1·5)	O(4^i)–N(2^i)–O(6^i)	117·6 (4)	120·5 (1·4)	O(7^i)–N(3^i)–O(9^i)	119·0 (4)	115·4 (1·0)
O(2^i)–N(1^i)–O(3^i)	125·5 (6)	124·7 (1·5)	O(5^i)–N(2^i)–O(6^i)	120·8 (4)	119·9 (1·5)	O(8^i)–N(3^i)· O(9^i)	120·0 (5)	114·2 (1·6)

shown in Table 2. The average N–O bond lengths and O–N̂–O bond angles are 1·25 (1) Å and 119 (1)° at 298 K, and 1·20 (1) Å and 119 (2)° at 403 K.

Discussion

The crystal structure of $RbNO_3$(IV), determined at 298 and 403 K, is consistent with the observed physical properties of piezoelectricity, pyroelectricity and optical activity. The structures at both temperatures are very similar, but there are some major differences in the magnitudes of the extinction and thermal parameters.

The extinction-parameter magnitudes suggest that the crystals used had close to 'ideally perfect' crystallinity at 298 K and close to 'ideally imperfect' crystallinity at 403 K. If this were so, the increase of crystal temperature may have caused the gradual conversion of crystallinity from its state at room temperature to being close to 'ideally imperfect' at

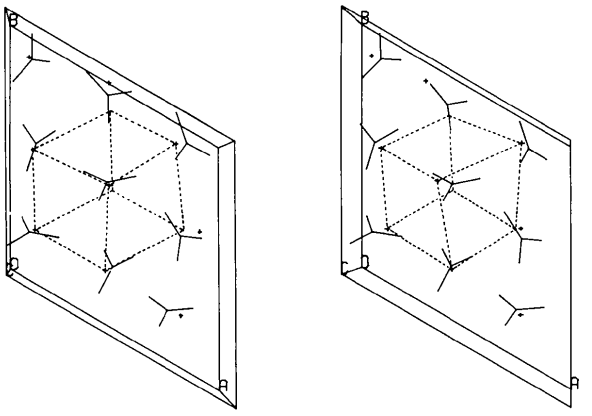

Fig. 2. A stereoview ([001] out of the paper) of the unit-cell contents for $RbNO_3$(IV) at 298 K. A typical Rb-atom pseudo-cube is outlined.

about 353 K. Within this temperature (rise) interval, the relative increase of the integrated intensities for strong, low-index reflections due to the change of 'crystal perfection' would likely be considerably greater than the relative decrease of intensities due to the temperature-factor effects. This could account for the increase of intensities with temperature rise to maxima values, while beyond this region the observed decrease of intensities could be due to the temperature-factor effects alone (Fig. 1*a*). On subsequent cooling from 438 K, the intensities increased continuously down to room temperature, as would be expected for the temperature-factor effects alone (Fig. 1*b*), and would be consistent with the crystal now being closer to 'ideally imperfect'.

The authors wish to express their thanks to the Australian Institute of Nuclear Science and Engineering (AINSE) and the Australian Atomic Energy Commission (AAEC) for use of their facilities. The receipt of an AINSE Grant is also gratefully acknowledged.

References

BROWN, R. N. & MCLAREN, A. C. (1962). *Acta Cryst.* **15**, 974–976.

BURY, P. C. & MCLAREN, A. C. (1969). *Phys. Status Solidi*, **31**(2), 799–806.

FRANKLIN, F. Y. W. & COX, D. E. (1970). *Acta Cryst.* A**26**, 377–378.

HETTICH, A. & STEINMETZ, H. (1932). *Z. Phys.* **76**, 688–706.

International Tables for X-ray Crystallography (1974). Vol. IV, p. 323. Birmingham: Kynoch Press.

KARPOV, S. V. & SHULTIN, A. A. (1970). *Phys. Status Solidi*, **39**, 33–38.

KENNARD, C. H. L. (1978). Private communication, Chemistry Department, University of Queensland. (Information conveyed from S. C. KENNEDY and M. R. SNOW.)

LUCAS, B. W. (1976). *J. Phys. E*, **9**, 262–264.

MUELLER, M. H., SIDHU, S. S., HEATON, L., HITTERMAN, R. L. & KNOTT, H. W. (1963). Report ANL-6797, p. 393. Argonne National Laboratory, Illinois.

NIMMO, J. K. (1980). *Acta Cryst.* A**36**, 830.

PAULING, L. & SHERMAN, J. (1933). *Z. Kristallogr.* **84**, 213–216.

PLYUSCHEV, V. E., MARKINA, I. B. & SHKLOVER, L. P. (1956). *Dokl. Akad. Nauk SSSR*, **108**, 645–647.

SCHNEIDER, C. S. (1976). *Acta Cryst.* A**32**, 375–379.

SHULL, G. G. & WOLLAN, E. O. (1956). *Solid State Phys.* **2**, 144.

Acta Cryst. (1982). B**38**, 2357–2361

The Structure of Ditin(II) Oxide Sulfate

BY GEORG LUNDGREN, GUNNAR WERNFORS AND TOSHIO YAMAGUCHI

Department of Inorganic Chemistry, Chalmers University of Technology and the University of Göteborg, S-412 96 Göteborg, Sweden

(*Received* 5 *February* 1982; *accepted* 5 *April* 1982)

Abstract

Sn_2OSO_4 crystallizes in the tetragonal space group $P42_1c$ with $a = 10{\cdot}930\ (2)$, $c = 8{\cdot}931\ (2)$ Å, $V = 1067\ (2)$ Å^3 and $Z = 8$. The structure has been refined to a final $R = 0{\cdot}049$ for 1796 significant diffractometer reflections. A three-dimensional structure is built up by the linkage of $Sn_8O_4^{8+}$ groups through sulfate ions. The two independent Sn atoms have an O coordination intermediate between three- and fourfold, both having three shorter Sn–O bonds in the range 2·137 (6)–2·353 (6) Å, and one longer of 2·523 (8) and 2·562 (8) Å, respectively. The sulfate group has S–O distances in the range 1·448 (8)–1·488 (7) Å.

0567-7408/82/092357-05$01.00